

Discussion Paper No.342

The Chaotic Monopolist Revisited with
Bounded Rationality and Delay Dynamics

Akio Matsumoto
Chuo University

Ferenc Szidarovszky
Corvinus University

January 2021



INSTITUTE OF ECONOMIC RESEARCH
Chuo University
Tokyo, Japan

The Chaotic Monopolist Revisited with Bounded Rationality and Delay Dynamics*

Akio Matsumoto[†] Ferenc Szidarovszky[‡]

Abstract

Two types of boundedly rational monopolists are studied when the marginal revenue is not necessarily negative sloping. Knowledgeably monopolists (k -monopolists) know the analytic form of the price function but unable to compute the profit-maximizing output level. Limited monopolists (ℓ -monopolists) know only the price and output values in two previous time periods. It is assumed that k -monopolists adjust their output levels according to the usual gradient process, while ℓ -monopolists approximate the marginal profit with a two-point finite difference formula. Discrete and continuous time scales are examined. A single-delay model is considered for k -monopolists, however for ℓ -monopolists a two-delay model is constructed. In the discrete case the stability condition is the same for the two models and requires a sufficiently small speed of adjustments. However, there are differences in the two dynamics. In the continuous case the discrete models are transformed into continuous models via Berezowski transformation. In the one delay case the critical values of the delays are computed and the directions of stability switching determined. In the two-delay case the stability switching curves are analytically found and the directions of stability switchings are characterized by computing the stability index for each point of the curves. The analytical results are verified and illustrated via numerical studies, when sensitivity analysis is performed showing that an increase in the adjustment coefficient shrinks the stability region, while it is extended by increasing the inertia coefficient.

Keywords: Boundedly rational monopolist, Delay differential equation, Gradient dynamics, Hopf bifurcation, Continuous and discrete models

*The first author highly acknowledges the financial support from the Japan Society for the Promotion of Science (Grant-in-Aid for Scientific Research (C) 20K01566).

[†]Department of Economics, Chuo University, 742-1, Higashi-Nakano, Hachioji, Tokyo, 192-0393, Japan, akiom@tamacc.chuo-u.ac.jp.

[‡]Department of Mathematics, Corvinus University, Budapest, Fővám tér 8, 1093, Hungary, szidarka@gmail.com.

1 Introduction

A textbook monopoly theory implicitly assumes that a monopolist possesses (i) perfect knowledge of the price function, (ii) the enough computability to make its optimal choices and (iii) instantaneous information about the economic activities in the market. Further, the price function is assumed to be (iv) linear. Consequently, the textbook monopolist can solve the profit maximization condition to determine a unique monopoly output and set the corresponding monopoly price on the price function to clear the market. Such a monopolist is called a *rational monopolist* that is a profit-maximizer and a price-maker. Since the rational monopolist can hit on the exact point at which its profit is maximized and jump to it with a one-shot, the theory does not involve any dynamic consideration.

In the old literature, Robinson (1933) is critical for a linear shape of the price function and emphasizes that a nonlinear price function is plausible in the market where there are several groups of consumers and each possesses a different level of income. In such an environment, even if the price curve is downward-sloping, the marginal revenue curve takes a convex-concave shape generating multiple monopoly states. A monopolist with imperfect knowledge somehow arrives at one of them but have no incentive to move further, although it possibly gains a larger profit at some other point. No one doubts the importance of limited information, uncertainty, and non-instantaneous response for optimal decision making. However, little has been done to develop the existing monopoly theory.¹

In recent literature, some studies have been conducted on the optimal behavior of a *boundedly rational monopolist* that lacks some or all requirements (i), (ii), (iii) and (iv). This development gives rise to a natural question: what happens if such a monopolist sets its output at some level other than the monopoly output level? Puu (1995) reproduces Robinson's verbal model faithfully and mathematically with a cubic price function having the inflection point. It is demonstrated that complicated output dynamics can arise when the monopolist adopts the gradient adjustment based on the past realized profits in discrete-time scales. Further, assuming that the price function is hyperbolic or log-concave, Naimzada and Ricchiuti (2008), Askar (2013) and Elsadany and Awad (2016) construct the discrete-time output adjustment process of the boundedly rational monopolist and numerically exhibit chaotic output evolution. Matsumoto and Szidarovszky (2014) examine discrete and one-delay monopoly dynamics with special binomial price and cost functions, when the dynamic equation includes an inertia coefficient. Only recently, Matsumoto and Szidarovszky (2020) reexamine this model in a continuous-time framework under the conditions that the price function is hyperbolic.

In this study, we return to Puu (1995) and reconsider, in a new apparatus of delay differential equation, Robinson's insight that the marginal revenue curve is not necessarily negative-sloping and the monopolist does not know all about

¹Basic elements of today's theory can be found in Robinson (1933) and Hicks (1935).

the market. To proceed, we introduce two boundedly rational monopolists. It is first assumed that neither of them has enough computability to calculate the monopoly output level. Besides, the monopolist is referred to as "knowledgeable" if it has full information on the form of the price function and "limited" if it does not know the form of the price function but possesses the values of output and price only in the past two periods. We call the former the *k-monopolist* and the latter the *ℓ-monopolist* for convenience. Concerning the output level's determination, we adopt the gradient method based on observing a profit change per unit output change. In the existing literature, it is not yet revealed whether the stability conditions for the *k-monopolist* and the *ℓ-monopolist* are the same or not. It is not fully discussed whether delayed information could be a source of output oscillations when the stability conditions are violated. Hence, this paper compares the dynamic behavior of these two monopolists and discuss the similarities and differences between them.

The paper is organized as follows. Section 2 constructs a basic monopoly model. Section 3 reviews the local and global dynamics in discrete-time scales. Section 4 builds two continuous time models that correspond to the discrete-time model. It is the central part of this paper and is divided into three subsections. The dynamics for the *k-monopolist* and for *ℓ-monopolist* is considered in the first and second subsections. A comparison between the dynamics of the two monopolists is made in the third. Section 5 offers conclusions and outlines further research directions.

2 Basic Models

Consider a monopolist that produces the quantity of output x . The price and cost functions are denoted as $p(x)$ and $c(x)$. The profit function is defined as a difference of the revenue from the production cost,

$$\pi(x) = p(x)x - c(x). \quad (1)$$

The profit-maximization condition for an interior solution is

$$\frac{d\pi}{dx} = 0 \quad (2)$$

and the market-clearing condition is to determine a price on the price function,

$$p = p(x). \quad (3)$$

A textbook monopolist or rational monopolist can solve the profit-maximization condition (2) to determine its monopoly output x_M and set a monopoly price p_M through (3).

Our interest is focused on a boundedly rational monopolist that cannot make such an optimal decision due to insufficient information. We formally define two monopolists depending on how much information they have. If a monopolist has full knowledge of the market price and cost functions but lacks the full

computability, it is called the *knowledgeable* monopolist or the *k*-monopolist. If a monopolist has neither of requirements (i) and (ii) but knows the values of x and p in the past two periods of time, then it is called the *limited* monopolist or the ℓ -monopolist. Since each monopolist is unable to solve the first-order condition (2) of the profit maximization, it determines an output level by checking whether a small change in the current output will increase or decrease their profits. If the profit is expected to increase, decrease or remain the same, then the monopolist increases, decreases and maintains the current level, accordingly. The *k*-monopolist knows the form of the marginal profit. Hence it will adjust output according to the following rule in discrete-time scales,

$$x(t) = x(t-1) + K \frac{d\pi(t-1)}{dx(t-1)} \quad (4)$$

where K is the adjustment coefficient and assumed to be positive. Alternatively, the ℓ -monopolist observes only the profits $\pi(t-1)$ and $\pi(t-2)$ with output levels $x(t-1)$ and $x(t-2)$ in the immediate past two periods. Based on this information, it determines the next output level as

$$x(t) = x(t-1) + K \frac{\pi(t-1) - \pi(t-2)}{x(t-1) - x(t-2)}. \quad (5)$$

The solutions of these dynamic equations give the output behavior over time. Note that information acquisition requires some time-delays in the discrete-time framework. The formula (4) is called the gradient method and is often used to explore the dynamics of the boundedly rational monopolist.²

In this section, we recapitulate a basic structure of Puu (1995) that reconsiders Robinson (1933). The price function is cubic,

$$p(x) = A - Bx + Cx^2 - Dx^3. \quad (6)$$

The revenue is $R(x) = p(x)x$ and thus the marginal revenue is also cubic,

$$MR(x) = A - 2Bx + 3Cx^2 - 4Dx^3. \quad (7)$$

It is further assumed that the cost function is cubic in x and has no fixed cost,

$$K(x) = Ex - Fx^2 + Gx^3$$

and then the marginal cost is quadratic,

$$MC(x) = E - 2Fx + 3Gx^2. \quad (8)$$

The profit function becomes quartic and is simplified as

$$\pi(x) = ax - bx^2 + cx^3 - dx^4 \quad (9)$$

²See, Naimzada and Ricchiuti (2008), Askar (2013), Elsadany and Awad (2016)). The adjustment process of (5) is considered in Puu (1995) and Matsumoto and Szidarovszky (2021)

with

$$a = A - E, \quad b = B - F, \quad c = C - G, \quad \text{and} \quad d = D$$

The marginal profit is

$$\frac{d\pi}{dx} = a - 2bx + 3cx^2 - 4dx^3. \quad (10)$$

Solving $d\pi/dx = 0$ yields the profit maximizing output levels. The number of the optimal solutions depends on the parameter specification and is one or three. Puu (1995) assumes the following parameter specification,

Assumption I. $a = 3.6$, $b = 2.4$, $c = 0.6$ and $d = 0.05$.

Equating the marginal profit to zero and solving it yield three real solutions,

$$x_1^e = 3 - \sqrt{3}, \quad x_2^e = 3 \quad \text{and} \quad x_3^e = 3 + \sqrt{3} \quad (11)$$

The corresponding profits are

$$\pi(x_1^e) = \pi(x_3^e) = \frac{9}{5} \quad \text{and} \quad \pi(x_2^e) = \frac{27}{20}$$

where $\pi(x_1^e)$ and $\pi(x_3^e)$ are the (local) maximum profit values and $\pi(x_2^e)$ is the (local) minimum profit value. Figure 1 illustrates the price curve, the marginal profit curve and the marginal cost curve, which is a reproduction of Figure 1 of Puu (1995) intended to duplicate Figure 22 of Robinson (1933). In our framework, both monopolists lack enough computability to find the optimal values and do not know the existence of multiple optimal outputs. Having their own information, the monopolists determine their production decisions based on the gradient of the marginal profit changes. The two main questions we are confronted with are the followings:

- (i) Under what condition can the monopolist arrive at the optimal (profit-maximizing) solution?
- (ii) Where does the monopolist go when it is unable to reach the optimal

solution?

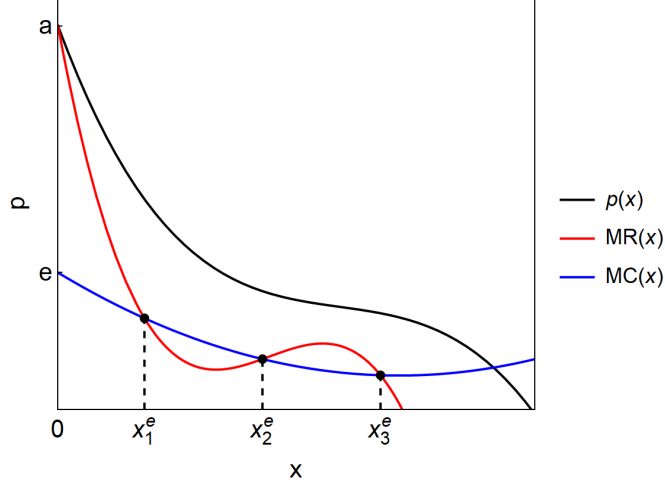


Figure 1. Price curve, MR and MC curves

3 The Discrete-Time Models

In the discrete-time scales, Puu (1995) has considered the dynamic behavior of the ℓ -monopolist that knows only the two points on the price function. It cannot calculate the marginal profit but obtains a proxy for it by a two-point divided difference formula:

$$\frac{\Delta\pi}{\Delta x} = \frac{\pi[x(t-1)] - \pi[x(t-2)]}{x(t-1) - x(t-2)} \quad (12)$$

where the right-hand side is equal to the following,

$$a - b[x(t-1) + x(t-2)] + c[x^2(t-1) + x(t-1)x(t-2) + x^2(t-2)] - d[x^3(t-1) + x^2(t-1)x(t-2) + x(t-1)x^2(t-2) + x^3(t-2)]$$

and is denoted as $g[x(t-1), x(t-2)]$. Hence, the searching process of the ℓ -monopolist (5) can be described by a second-order difference equation,

$$x(t) = x(t-1) + Kg[x(t-1), x(t-2)]. \quad (13)$$

We also examine the k -monopolist dynamic behavior for comparison. Since the k -monopolist knows the price and cost functions and thus the marginal profit, (10), its output is determined by a first-order non-linear difference equation,

$$x(t) = x(t-1) + Kf[x(t-1)] \quad (14)$$

where

$$f(x) = \frac{d\pi}{dx} = a - 2bx + 3cx^2 - 4dx^3$$

Notice that each of the equilibrium outputs x_i^e for $i = 1, 3$ is a stationary output for both dynamic systems, (13) and (14). The stability condition for (14) is

$$\left| \frac{dx(t)}{dx(t-1)} \right| = |1 - 2\alpha K| < 1 \quad (15)$$

that is

$$K < \frac{1}{\alpha}$$

where, under Assumption I,

$$\alpha = b - 3cx_i^e + 6d(x_i^e)^2 = \frac{3}{5} \text{ for } i = 1, 3.$$

The characteristic polynomial of the homogeneous part corresponding to (13) is

$$\varphi(\lambda) = \lambda^2 - (1 - \alpha K)\lambda + \alpha K$$

where

$$\frac{\partial g}{\partial x(t-1)} = \frac{\partial g}{\partial x(t-2)} = -\alpha.$$

The stability conditions for a quadratic equation are

$$\varphi(1) = 2\alpha K > 0, \quad \varphi(-1) = 2 > 0 \text{ and } 1 - \alpha K > 0. \quad (16)$$

From (15), the absolute value of the slope of (14) at the stationary output is less than unity if $K < 1/\alpha$. Since the first two conditions in (16) always hold, the stability of system (13) is assured if the last inequality is satisfied, $K < 1/\alpha$. Hence, local stability of the stationary output are summarized as follows:

Theorem 1 *Given Assumption I, the optimal outputs, x_1^e and x_3^e , are locally asymptotically stable in both dynamic equations (13) and (14) if $K < 1/\alpha$.*

We now investigate how the output globally evolves when the adjustment parameter K is continuously changed. Under Assumption I, Figure 2(A) shows two bifurcation diagrams when the initial point is selected around the larger equilibrium x_3^e .³ The red bifurcation diagram is for the k -monopolist and the blue one for the ℓ -monopolist. The bifurcation parameter K has been increased in steps of 0.007 from 0.1 to $K_1 = 3.335$ for the red diagram and to $K_2 = 3.58$ for the blue one. Trajectories for K larger than those critical values eventually take negative values and thus lose their economic meanings. For each value of K , dynamic systems (13) and (14) are iterated 2000 times and the output data

³We obtain a symmetric bifurcation diagram with respect to the $x = x_2^e$ line when an initial point is selected in the neighborhood of x_1^e . This is because the profit function is symmetric with respect to $x = x_2^e$.

for the last 100 iterations are plotted against K . It is confirmed in Figure 2(A) that the equilibrium x_3^e is asymptotically stable for $K < K_0 = 5/3$. Figure 2(B) describes two time trajectories starting at the same initial point, $x(0) = x_3^e + 0.5$ with $K = 1.6$ in which the red one is for the k -monopolist and the blue one for the l -monopolist. Although it will take more time than the k -monopolist, the l -monopolist having only very limited information can arrive at the equilibrium when it adopts cautious adjustments with a smaller value of K .

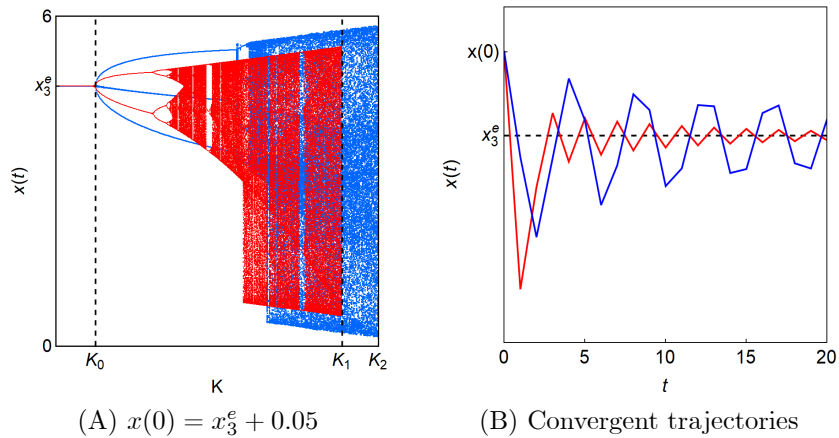


Figure 2. Bifurcation diagram and time trajectories for the two monopolists

We present some numerical results concerning the global dynamics of (13) and (14) when the equilibrium x_3^e becomes unstable. The time-trajectory starting in the neighborhood of x_3^e is illustrated in red and that starting around x_1^e in blue. The first results are obtained for $K = 2.1$. The red bifurcation diagram in Figure 2(A) shows that the equilibrium becomes unstable and a new stable period-4 cycle is created after a stable period-2 cycle loses stability. Figure 3(A) illustrates a phase diagram of the periodic cycle surrounding the higher and lower intersections of the convex-concave curve, $x(t) = f[x(t-1)]$ and the diagonal, $x(t) = x(t-1)$. In Figure 3(B), the loci of $g[x(t-1), y(t-1)] = 0$ consist of the negative-sloping curve and the cycle-wise curve. The blue bifurcation diagram in Figure 2(A) seems to imply the birth of a period-3 cycle after stability loss. However, as shown in Figure 3(B), a period-4 cycle emerges. Observing the red diamond-shape cycle in the upper-right corner, the left and right points' ordinates are 4.58552 and 4.57699 after 500 iterations and thus their difference is almost invisible. The same result is obtained for the blue one

in the lower-left corner.

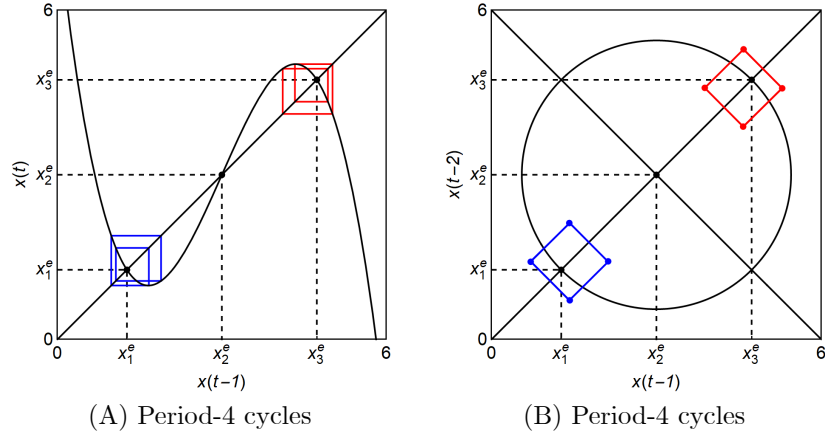


Figure 3. Periodic cycles

In the next examples, K takes different values and the situation becomes a bit complicated. K is increased to 2.6 in Figure 4(A) in which, after infinitely many bifurcations occur, chaotic output dynamics is possible, but the attractor is contained in two disjoint intervals. K is increased to 2.75 in Figure 4(B) which shows two coexisting chaotic attractors.

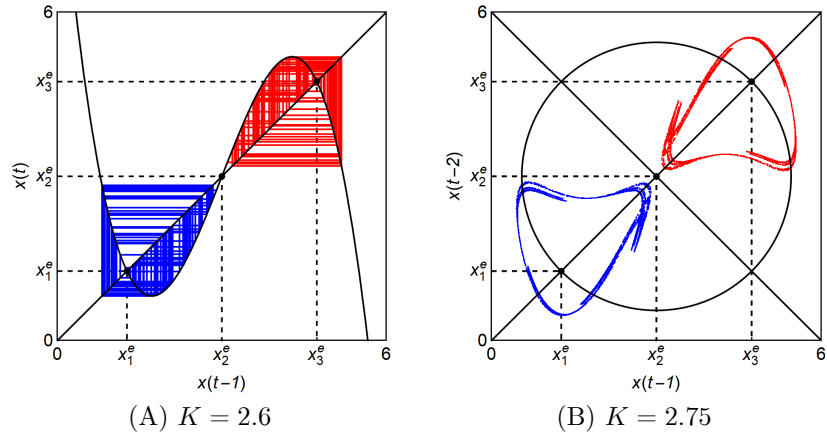
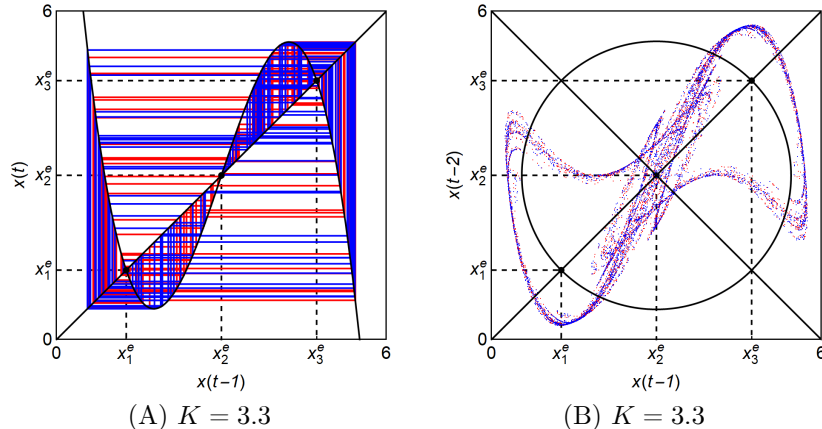


Figure 4. Separated chaotic dynamics

In the case of $K = 3.3$, the situation is much more complicated. In both of Figures 5(A) and 5(B), the chaotic attractors with smaller K merge into one

attractor. Time trajectories erratically oscillate over the entire domain.



33

Figure 5. Merged chaotic dynamics

There are some differences between the two monopolists. The red bifurcation diagram reveals that the dynamics is transformed into chaotic oscillation through a typical period-doubling cascade having windows. The blue bifurcation diagram displays a jump to chaos from periodic-oscillations. Figures 3-5 also exhibit similarities; periodic-cycles appear after losing stability, attractors of chaotic dynamics are first separated and then merged into one as K is increased.

4 Continuous-Time Models: Berezowski Transition

In this section, we transform a difference equation into a continuous equation and shed light on the roles of time delays in dynamics, addressing the following question: what can be said about the local and global dynamics when obtaining information needs some delays in continuous-time framework. There are many ways to transform a discrete-time model to a continuous-time model. Euler approximation is frequently used. Despite it, we adopt the method used by Berezowski (2001) and assume that the difference equations (13) for the ℓ -monopolist and (14) for the k -monopolist are connected with some physical process of definite inertia and rewrite these as continuous ones in the following ways;

$$\delta \dot{x}(t) + x(t) = x(t - \tau_1) + Kg[x(t - \tau_1), x(t - \tau_2)] \quad (17)$$

and

$$\delta \dot{x}(t) + x(t) = x(t - \tau) + Kf[x(t - \tau)] \quad (18)$$

where the fixed time interval of the discrete-time equation is replaced with the time delays, τ_1 , τ_2 and τ .⁴ The equilibrium outputs x_i^e for $i = 1, 3$ are stationary points of these equations and taking $\delta = 0$ can reduce (17) and (18) to the original discrete-time models. These delay continuous-time models have three essential factors that affect dynamics, the inertia coefficient δ , the adjustment coefficient K and the time delays, τ_1 , τ_2 and τ . We first investigate the local stability of the k -monopolist's dynamics equation (18) and then turn to the ℓ -monopolist's dynamic equation (17).

4.1 Continuous Model for the k -monopolist

To examine the local stability of the k -monopolist, we linearize the nonlinear equation (18) around the equilibrium output,

$$\delta \dot{x}(t) + x(t) - (1 - 2\alpha K)x(t - \tau) = 0 \quad (19)$$

where

$$\frac{\partial f}{\partial x(t-1)} = -2\alpha.$$

The corresponding characteristic equation based on an exponential solution, $x(t) = e^{\lambda t}u$, $u \neq 0$, is

$$\delta \lambda + 1 - (1 - 2\alpha K)e^{-\lambda \tau} = 0. \quad (20)$$

Since the real solution $\lambda = 0$ does not solve this equation, we assume the imaginary solution $\lambda = i\omega$, $\omega > 0$.⁵ With it, the characteristic equation can be separated into the real and imaginary parts,

$$\begin{aligned} 1 - (1 - 2\alpha K)\cos\omega\tau &= 0, \\ \delta\omega + (1 - 2\alpha K)\sin\omega\tau &= 0. \end{aligned} \quad (21)$$

Moving the constants of both equations to the right-side, squaring and adding them present

$$\omega^2 = \frac{4\alpha K(\alpha K - 1)}{\delta^2}. \quad (22)$$

Although $\alpha > 0$ and $K > 0$, $\omega^2 \leq 0$ if $\alpha K \leq 1$. In other words, there is no $\omega > 0$ that means no existence of pure imaginary solutions. Hence, no stability switch occurs. In addition, if $\tau = 0$, then (19) is reduced to

$$\delta \dot{x}(t) = -2\alpha Kx(t).$$

$\alpha K/\delta > 0$ leads to the local asymptotical stability in the no-delay case. These results, therefore, imply that the delay is *harmless* and is summarized as follows:

⁴If we take Euler approximation, $\dot{x}(t) = x(t) - x(t-1)$, then (13) and (14) are reduced to

$$\dot{x}(t) = Kg[x(t - \tau_1), x(t - \tau_2)]$$

and

$$\dot{x}(t) = Kf[x(t - \tau)].$$

With these equations, we can proceed the analysis as in the same way to be done below.

⁵A conjugate pair can also be a solution. We only should consider positive ω .

Theorem 2 *If $\alpha K \leq 1$, then the optimal outputs x_i^e for $i = 1, 3$ of (18) are locally asymptotically stable for any $\tau \geq 0$.*

Alternatively, if $\alpha K > 1$, then ω^2 in (22) is positive and thus local stability can be violated. In particular, solving (22) for ω gives a positive solution,

$$\omega_+ = \frac{2\sqrt{\alpha K(\alpha K - 1)}}{\delta} > 0$$

that is substituted into the first equation of (21) to have

$$\cos\left(\frac{2\tau\sqrt{\alpha K(\alpha K - 1)}}{\delta}\right) = \frac{1}{1 - 2\alpha K}. \quad (23)$$

Solving (23) for τ yields the critical values of delay τ ,⁶

$$\tau_m(\delta, K) = \frac{\delta}{2\sqrt{\alpha K(\alpha K - 1)}} \left[\cos^{-1}\left(\frac{1}{1 - 2\alpha K}\right) + 2m\pi \right] \text{ for } m \in \mathbb{Z}^+. \quad (24)$$

Since the characteristic solution of (20) depends on delay, differentiating it gives

$$\delta \frac{d\lambda}{d\tau} - (1 - 2\alpha K) e^{-\lambda\tau} \left(-\tau \frac{d\lambda}{d\tau} - \lambda \right) = 0$$

or

$$\frac{d\lambda}{d\tau} = -\frac{(1 - 2\alpha K) e^{-\lambda\tau} \lambda}{\delta + (1 - 2\alpha K) e^{-\lambda\tau} \tau}.$$

With $(1 - 2\alpha K) e^{-\lambda\tau} = 1 + \delta\lambda$ from (20), the derivative is

$$\frac{d\lambda}{d\tau} = -\frac{(1 + \delta\lambda) \lambda}{\delta + (1 + \delta\lambda) \tau}.$$

At $\lambda = i\omega$, its real part is

$$\operatorname{Re} \left[\frac{d\lambda}{d\tau} \Big|_{\lambda=i\omega} \right] = \frac{(\delta\omega)^2}{(\delta + \tau)^2 + (\delta\tau\omega)^2} > 0.$$

This inequality implies that the solutions crossing the imaginary axis at $i\omega$ cross it from left to right as τ increases. Hence, stability is lost at $\tau_0(\delta, K)$ via a Hopf bifurcation⁷ and stability cannot be regained for any larger value of τ . It is seen that all real parts of the characteristic solution are negative for $\tau < \tau_0(\delta, K)$ and one of them becomes zero for $\tau = \tau_0(\delta, K)$. Therefore, we have the following on delay dynamics of the k -monopolist:

⁶If ω_+ is substituted into the second equation of (21), we can obtain the same values in a different form.

⁷It is confirmed now that the characteristic equation has a pair of pure imaginary solutions and no other solutions with zero real parts exist and that the derivative of the real part for τ is positive at the optimal output. Hence a Hopf bifurcation can occur. See, for example, Rustichini (1989).

Theorem 3 *If $\alpha K > 1$, then the optimal outputs x_i^e for $i = 1, 3$ of (18) are locally stable for $\tau < \tau_0(\delta, K)$, loses stability at $\tau = \tau_0(\delta, K)$ and bifurcates to periodic oscillations for $\tau > \tau_0(\delta, K)$ where $m = 0$ in (24) leading to*

$$\tau_0(\delta, K) = \frac{\delta}{2\sqrt{\alpha K(\alpha K - 1)}} \cos^{-1} \left(\frac{1}{1 - 2\alpha K} \right).$$

We now consider how a parameter change affects the critical value of τ . From (24), we have the following derivatives with $\alpha K > 1$,

$$\frac{\partial \tau_0(\delta, K)}{\partial \delta} = \frac{1}{2\sqrt{\alpha K(\alpha K - 1)}} \cos^{-1} \left(\frac{1}{1 - 2\alpha K} \right) > 0$$

and

$$\frac{\partial \tau_0(\delta, K)}{\partial K} = - \frac{\delta \alpha \left[2\alpha K(\alpha K - 1) + \sqrt{\alpha K(\alpha K - 1)}(2\alpha K - 1)^2 \cos^{-1} \left(\frac{1}{1 - 2\alpha K} \right) \right]}{4(2\alpha K - 1)\alpha K(\alpha K - 1)^2} < 0.$$

These inequality directions imply that increasing δ extends the stability region and increasing K makes the critical value of τ smaller. That is, δ has the stabilizing effect and K has the destabilizing effect. For an appropriate K value with which the discrete model exhibits complex dynamics, the corresponding continuous model produces similar dynamics if δ takes sufficiently smaller values (i.e., the dominance of the K 's destabilizing effect). However, such oscillatory dynamics disappear if δ takes sufficiently larger values (i.e., the dominance of the inertia stabilizing effect). These are numerically checked. The parameters are taken to be $\tau = 1$, $K = 3$ and $\delta_0 \simeq 1.221$ in Figure 6(A) in which increasing δ simplifies dynamics via period-halving cascade, whereas $\tau = 1$, $\delta = 0.2$ and $K_0 \simeq 1.777$ in Figure 6(B) in which increasing K complicates dynamics via period-doubling cascade.⁸

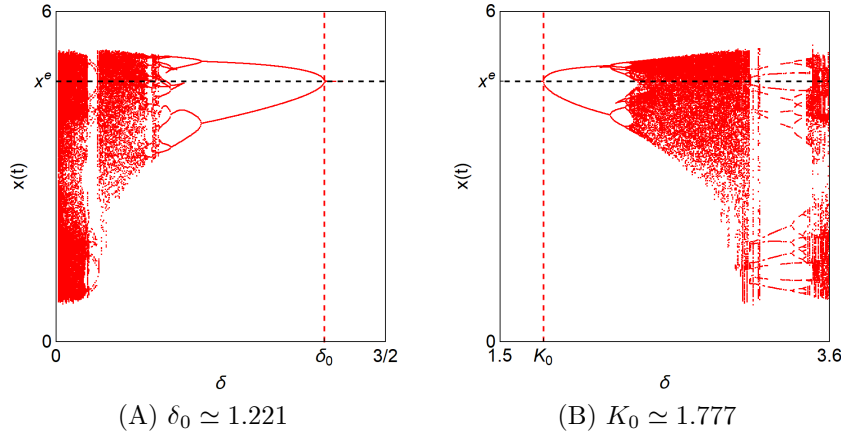


Figure 6. Bifurcation diagrams for δ and K with given value of τ

⁸Solving (24) for δ under given K and for K under given δ yield the critical values, δ_0 and K_0 , respectively.

To examine the time-delay effects, we perform some simulations for τ with different K -values and fixed value of $\delta = 0.2$. In Figure 7(A) with $K = 2.2$, the optimal point bifurcates to a limit cycle when it loses stability at $\tau = \tau_0 \simeq 0.343$. For further increased values of τ , a new multi-period cycle is created and then chaotic oscillations arise. A typical time trajectory exhibits regular alternative oscillations around higher and lower output levels. In Figure 7(B), the value of K is increased to 2.5 and accordingly, the critical τ value is decreased to $\tau_0 \simeq 0.242$. Chaotic oscillations around the equilibrium output appear after the *à la* period-doubling bifurcations. Two x -intervals including output oscillations in Figure 7(A) are merged to one as shown in Figure 7(B).

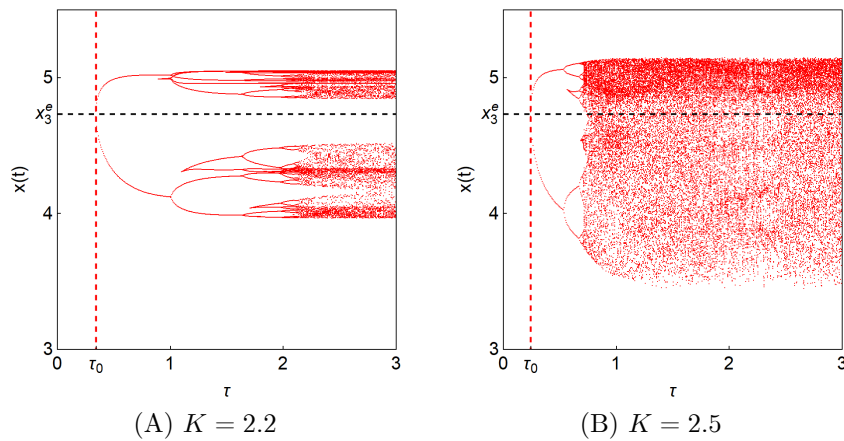


Figure 7. Bifurcation diagrams for τ with given values of δ and K

4.2 Continuous Model for the ℓ -monopolist

We now draw attention to dynamic equation (17) of the ℓ -monopolist. It is to be noticed that the optimal outputs x_i^e for $i = 1, 3$ are the stationary outputs for (17) and the inequality relation, $\tau_1 \leq \tau_2$, should hold since $x(t - \tau_1)$ is the newest output information obtained at $t - \tau_1$ and $x(t - \tau_2)$ is the second-newest at $t - \tau_2$. Linearizing (17) around the stationary output gives

$$\delta \dot{x}(t) + x(t) = (1 - \alpha K) x(t - \tau_1) - \alpha K x(t - \tau_2)$$

where, as in the difference equation,

$$\frac{\partial g}{\partial x(t - \tau_1)} = \frac{\partial g}{\partial x(t - \tau_2)} = -\alpha.$$

The stability of the linearized equation depends on the locations of the solutions of the associated characteristic equation. Substituting the exponential solution presents

$$\delta \lambda + 1 - (1 - \alpha K) e^{-\lambda \tau_1} + \alpha K e^{-\lambda \tau_2} = 0.$$

or dividing both sides by $1 + \delta\lambda$ gives the following form,

$$1 + a_1(\lambda)e^{-\lambda\tau_1} + a_2(\lambda)e^{-\lambda\tau_2} = 0 \quad (25)$$

where

$$a_1(\lambda) = -\frac{1 - \alpha K}{1 + \delta\lambda} \text{ and } a_2(\lambda) = \frac{\alpha K}{1 + \delta\lambda}.$$

As is seen, the characteristic equation depends on delays and hence its solutions also depend on delays. In consequence, as the values of delays change, the stability of stationary outputs may change accordingly. Such phenomena are called *stability switches*. The key technique determining those switches under two delays is fully discussed in Matsumoto and Szidarovszky (2018) and is applied for the two delay continuous model, (17).

Any stability switch might occur when the real part of the characteristic solution changes its sign from negative to positive (i.e., stability loss) or positive to negative (i.e., stability gain). It is clear that $\lambda = 0$ does not solve the characteristic equation (25). It is crucial to determine the values of τ_1 and τ_2 at which (25) has a pair of conjugate pure imaginary solutions. We then let $\lambda = i\omega$ with $\omega > 0$ and substitute it into (25),

$$1 + a_1(i\omega)e^{-i\omega\tau_1} + a_2(i\omega)e^{-i\omega\tau_2} = 0 \quad (26)$$

where

$$a_1(i\omega) = -\frac{1 - \alpha K}{1 + (\delta\omega)^2} + i\frac{(1 - \alpha K)\delta\omega}{1 + (\delta\omega)^2}$$

and

$$a_2(i\omega) = \frac{\alpha K}{1 + (\delta\omega)^2} - i\frac{\alpha K\delta\omega}{1 + (\delta\omega)^2}.$$

The absolute values and the arguments of $a_1(i\omega)$ and $a_2(i\omega)$ are, respectively, given as follows,

$$|a_1(i\omega)| = \frac{|1 - \alpha K|}{\sqrt{1 + (\delta\omega)^2}}, \quad |a_2(i\omega)| = \frac{\alpha K}{\sqrt{1 + (\delta\omega)^2}} \quad (27)$$

and

$$\arg[a_1(i\omega)] = \arg[a_2(i\omega)] = -\tan^{-1}(\delta\omega) + 2\pi \quad (28)$$

We now solve equation (26) in which the three terms are considered three vectors in the complex plane. Their magnitudes are 1, $|a_1(i\omega)|$ and $|a_2(i\omega)|$. The right hand side of (26) is zero, implying that if we put these vectors head to tail, they form a triangle (Figure 8). The imaginary solution $\lambda = i\omega$ with $\omega > 0$ can solve (26) for some τ_1 and τ_2 if and only if the following triangle conditions hold,⁹

$$1 \leq |a_1(i\omega)| + |a_2(i\omega)|$$

⁹See Proposition 3.1 of Gu et al (2005) showing that an imaginary solution is obtained if and only if the triangle conditions hold.

and

$$-1 \leq |a_1(i\omega)| - |a_2(i\omega)| \leq 1.$$

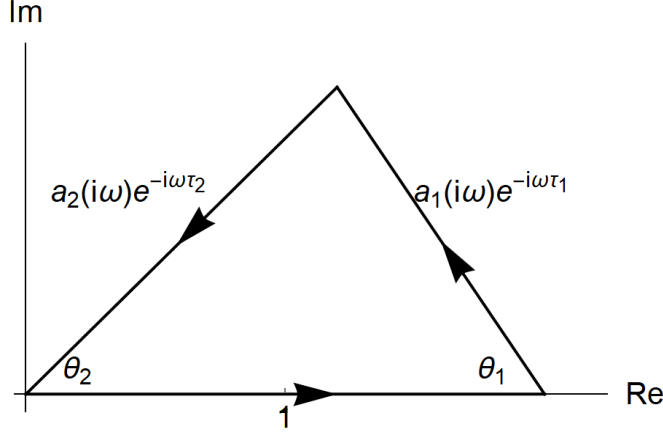


Figure 8. Triangle formed by three vectors

Depending on whether $\alpha K \leq 1$ or $\alpha K > 1$, we have the following two results.

Theorem 4 *If $\alpha K \leq 1$, then the optimal outputs x_i^e for $i = 1, 3$ of (17) are locally asymptotically stable for any $\tau_1 \geq 0$ and $\tau_2 \geq 0$.*

Proof. If $\alpha K \leq 1$, from (27),

$$|a_1(i\omega)| + |a_2(i\omega)| = \frac{1}{\sqrt{1 + (\delta\omega)^2}} < 1.$$

One of the triangle conditions is violated (that is, a triangle is not constructed), implying that no pure imaginary solutions solve (26) for any τ_1 and τ_2 . The optimal output is locally asymptotically stable for $\tau_1 = \tau_2 = 0$. Hence, it is stable for any τ_1 and τ_2 since no stability switch occurs. ■

The other result is concerned with the critical values of the delays:

Theorem 5 *If $\alpha K > 1$ and $\delta\omega \leq 2\sqrt{\alpha K(\alpha K - 1)}$, then the characteristic equation (17) with $\tau_1 > 0$ and $\tau_2 > 0$ has pure imaginary solutions for the following sets of the delays,*

$$\tau_{1,m}^{\pm}(\omega) = \frac{1}{\omega} [\arg[a_1(i\omega)] + (2m - 1)\pi \pm \theta_1(\omega)] \text{ for } m \in \mathbb{Z}^+,$$

$$\tau_{2,n}^{\mp}(\omega) = \frac{1}{\omega} [\arg[a_2(i\omega)] + (2n - 1)\pi \mp \theta_2(\omega)] \text{ for } n \in \mathbb{Z}^+$$

where

$$\theta_1(\omega) = \cos^{-1} \left(\frac{(\delta\omega)^2 + 2(1 - \alpha K)}{2(\alpha K - 1)\sqrt{1 + (\delta\omega)^2}} \right) \text{ and } \theta_2(\omega) = \cos^{-1} \left(\frac{(\delta\omega)^2 + 2\alpha K}{2\alpha K\sqrt{1 + (\delta\omega)^2}} \right)$$

Proof. It can be checked that the triangle conditions are satisfied if $\alpha K > 1$ and $\delta\omega \leq 2\sqrt{\alpha K(\alpha K - 1)}$. The internal angles θ_1 and θ_2 of the triangle are calculated by the law of cosine. For the vectors $a_1(i\omega)e^{-i\omega\tau_1}$ and $a_2(i\omega)e^{-i\omega\tau_2}$, we have the followings, noticing that a symmetric triangle can be formed above and under the real axis in Figure 8,

$$\arg [a_1(i\omega)e^{-i\omega\tau_1}] \pm \theta_1(\omega) + 2m\pi = \pi, \quad m \in \mathbb{Z}^+$$

and

$$\arg [a_2(i\omega)e^{-i\omega\tau_2}] \mp \theta_2(\omega) + 2n\pi = \pi, \quad n \in \mathbb{Z}^+.$$

With $\arg [e^{-i\omega\tau_k}] = -\omega\tau_k$, the forms of $\tau_{1,m}^\pm(\omega)$ and $\tau_{2,n}^\mp(\omega)$ are obtained. ■

We can numerically confirm the stabilizing effect of δ for a fixed value of K and the destabilizing effect of K for a fixed value of δ . Given $\tau_{1,0}^- = 1$ and $\tau_{2,0}^+ = 2$, the critical values, $\delta_0 \simeq 1.674$ in Figure 9(A) and $K_0 \simeq 1.727$ in Figure 9(B), are obtained by solving the following simultaneous equations with $K = 3$, respectively, with $\delta = 0.2$,¹⁰

$$\omega\tau_{1,0}^- = -\tan^{-1}[\delta\omega] + \pi - \theta_1(\omega),$$

$$\omega\tau_{2,0}^+ = -\tan^{-1}[\delta\omega] + \pi + \theta_2(\omega).$$

As is seen, dynamics generated by (17) are simplified when δ is increased and is complicated when K is increased. It is interesting to observe that the shapes of the bifurcation diagrams constructed by decreasing δ or increasing K seem to be similar to the blue diagram obtained by increasing K in Figure 2(A)

¹⁰We solve these nonlinear equations with Mathematica, vol.12.1.

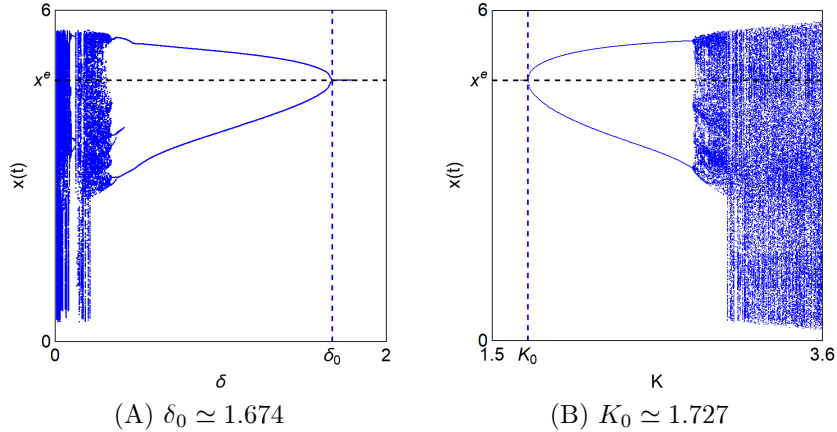


Figure 9. Bifurcation diagrams with respect to δ and K

We immediately obtain the followings from Theorem 5:

Theorem 6 *The stability switching curve consists of the following segments,*

$$SW_{m,n}^1 = \left\{ (\tau_{1,m}^+(\omega), \tau_{2,n}^-(\omega)) \mid \omega \in \left[0, \frac{2\sqrt{\alpha K(\alpha K - 1)}}{\delta} \right], (m, n) \in \mathbb{Z}^+ \right\}$$

$$SW_{m,n}^2 = \left\{ (\tau_{1,m}^-(\omega), \tau_{2,n}^+(\omega)) \mid \omega \in \left[0, \frac{2\sqrt{\alpha K(\alpha K - 1)}}{\delta} \right], (m, n) \in \mathbb{Z}^+ \right\}.$$

We now examine how the stability switching curve is shifted when the parameter δ or K changes. In Figure 10, $\tau_2 \geq \tau_1$ in the yellow region, the red, green, and blue curves are described by the segments $SW_{0,0}^2$, respectively, with $\delta = 0.2$ and $K = 1.75$, $\delta = 0.3$ and $K = 1.75$ and $\delta = 0.2$ and $K = 2$.¹¹ Let us take the red curve as a starting point. The red one divides the feasible yellow region into two subregions. It has been checked that the stationary point is locally asymptotically stable when there are no delays. In other words, the stability is preserved in the subregion including the origin of $\tau_1 = \tau_2 = 0$. Hence, the lower part of the yellow region is the stability region. The stability is lost when a pair of two delays crosses the stability switching curve. When the value of δ is increased, the red curve is shifted rightward to the green curve, enlarging the stability region. Hence, increasing δ has the stabilizing effect, which has been confirmed in Figure 9(A). However, when the K -value is increased, the

¹¹The corresponding dotted curves in the white region are described by the segment $SW_{0,0}^1$ with the same parameter specifications. However, the condition $\tau_1 \leq \tau_2$ is violated, and thus, these curves are not considered anymore.

red curve is shifted leftward to the blue curve, shrinking the stability region. Hence increasing K has the destabilizing effect, which has also been confirmed in Figure 9(B).

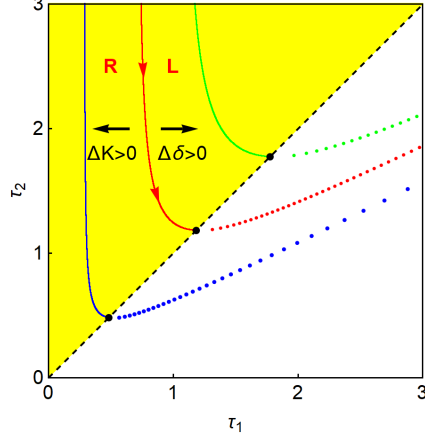


Figure 10. Stability switching curves

We calculate the stability index to find directions of stability switches and provide a theoretical background for numerically-determined directions of the stability switches.¹² The second vector in (26) is rewritten as

$$a_1(i\omega)e^{-i\omega\tau} = \left(-\frac{1-\alpha K}{1+(\delta\omega)^2} + i\frac{(1-\alpha K)\delta\omega}{1+(\delta\omega)^2} \right) (\cos\omega\tau_1 - i\sin\omega\tau_1).$$

Let R_1 and I_1 denote its real and imaginary parts,

$$\begin{aligned} R_1 &= -\frac{1-\alpha K}{1+(\delta\omega)^2} \cos\omega\tau_1 + \frac{(1-\alpha K)\delta\omega}{1+(\delta\omega)^2} \sin\omega\tau_1, \\ I_1 &= \frac{(1-\alpha K)}{1+(\delta\omega)^2} \sin\omega\tau_1 + \frac{(1-\alpha K)\delta\omega}{1+(\delta\omega)^2} \cos\omega\tau_1. \end{aligned} \quad (29)$$

Similarly, the third vector is

$$a_2(i\omega)e^{-i\omega\tau} = \left(\frac{\alpha K}{1+(\delta\omega)^2} - i\frac{\alpha K\delta\omega}{1+(\delta\omega)^2} \right) (\cos\omega\tau_2 - i\sin\omega\tau_2)$$

and the real part, R_2 , and the imaginary part, I_2 , are given by

$$\begin{aligned} R_2 &= \frac{\alpha K}{1+(\delta\omega)^2} \cos\omega\tau_2 - \frac{\alpha K\delta\omega}{1+(\delta\omega)^2} \sin\omega\tau_2, \\ I_2 &= -\frac{\alpha K}{1+(\delta\omega)^2} \sin\omega\tau_2 - \frac{\alpha K\delta\omega}{1+(\delta\omega)^2} \cos\omega\tau_2. \end{aligned} \quad (30)$$

¹²See Gu et al. (2005) for more detailed discussion.

The stability index is defined as follows:

$$S = R_2 I_1 - R_1 I_2.$$

With (29) and (30), S can be written as

$$S = -\frac{\alpha K (\alpha K - 1)}{1 + (\delta\omega)^2} \sin \omega (\tau_1 - \tau_2) \quad (31)$$

where we use the following relations: the coefficients of $\sin \omega \tau_1 \sin \omega \tau_2$ and $\cos \omega \tau_1 \cos \omega \tau_2$ are zero and those of $\sin \omega \tau_1 \cos \omega \tau_2$ and $\cos \omega \tau_1 \sin \omega \tau_2$ are, respectively,

$$-\frac{\alpha K (\alpha K - 1)}{1 + (\delta\omega)^2} \text{ and } \frac{\alpha K (\alpha K - 1)}{1 + (\delta\omega)^2}.$$

We call the direction of the curve that corresponds to increasing ω the *positive direction*. We also call the region on the left-hand side the *region on the left* when we head in the curve's positive direction. The *region on the right* is similarly defined. Concerning the stability switches, we have the following result from Matsumoto and Szidarovszky (2018).

Theorem 7 *Let (τ_1, τ_2) be a point on the stability switching curve. Assume we look toward increasing values of ω on the curve, and a point (τ_1, τ_2) moves from the region on the right to the region on the left. Then a pair of characteristic solutions crosses the imaginary axis to the right if $S > 0$ and to the left if $S < 0$.*

We now compute the stability index on the solid red stability switching curve in Figure 10. From Theorem 5, the red segment is the locus of the following points,

$$SW_{0,0}^2 = \left\{ (\tau_{1,0}^-(\omega), \tau_{2,0}^+(\omega)) \mid \omega \in \left[0, \frac{2\sqrt{\alpha K (\alpha K - 1)}}{\delta} \right] \right\}$$

where, by the definitions of the critical delays in Theorem 5,

$$\omega (\tau_{1,0}^-(\omega) - \tau_{2,0}^+(\omega)) = -[\theta_1(\omega) + \theta_2(\omega)] < 0.$$

With $\alpha K > 1$ and $\delta\omega > 0$, the stability index of (31) is positive. Hence, when a pair of (τ_1, τ_2) crossing the solid red segment from the region on the right denoted by **R** to the region on the left denoted by **L** in Figure 10, a pair of the corresponding characteristic solutions crosses the imaginary axis to the right from the left, implying stability loss. The same consideration can be applied to the stability index along the green and blue curves.

We draw attention to how the delay affects dynamics. We take $K = 2.2$ and $\tau_2 = 2$. Figure 11(A) illustrates a bifurcation diagram for $\tau_1 \in [0, \tau_2]$ and shows the birth of complicated dynamics for τ_1 a little bit larger than $\tau_0 \simeq 0.207$ and a little bit smaller than $3 (= \tau_2)$. A limit cycle appears for the medium

values of τ_1 . Figure 11(B) is an enlargement of Figure 11(A) around τ_0 and shows that multi-stability occurs. The red curve is the diagram with the initial function $\varphi(t) = x_3^e + 0.2$ for $t \leq 0$ and the blue curve is the diagram with the initial function $\varphi(t) = x_3^e + 0.01$. The two curves are different for τ_1 less than $\tau_1 = 0.5007$ and become identical for larger τ_1 . Figure 11(C) is the phase diagrams with $\tau_1 = 0.5007$, before merging the red curve and the blue curve. Multi-stability is observed when K is increased to 2.5 but is not found any more for $K = 3$.

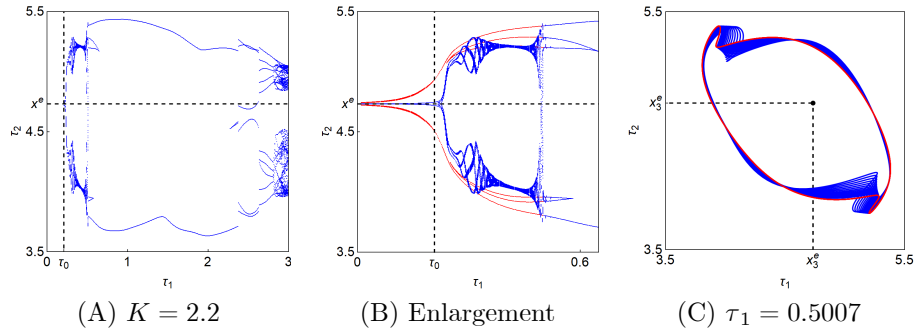


Figure 11. Bifurcation diagrams for τ_1

4.3 Comparison: Delay Dynamics

This subsection compares the delay effects caused by the two monopolists with larger values of K . For numerical simulations, we fix the value of the inertia coefficient $\delta = 0.2$, the adjustment coefficient $K = 3$ and $\tau_2 = 3$. It is then investigated how the dynamics change when the bifurcation parameters τ_1 of (17) and τ of (18) are increased. In numerical simulations, the initial functions associated with the dynamics equations are assumed to be identical, $\varphi(t) = x_3^e + 0.1$ for $t \leq 0$. Figures 12(A) and (B) illustrate the bifurcation diagrams with respect to τ and τ_1 , both of which are selected from the interval $[0.01, 3]$.¹³ The critical delay values for which the stability is violated are different: the stability loss of the ℓ -monopolist occurs at $\tau_0^\ell \simeq 0.1$ that is smaller than the critical value of the k -monopolist, $\tau_0^K \simeq 0.164$. After losing stability, the optimal output is replaced with periodic or aperiodic oscillations and the resultant diagrams are separated into two parts, one in which the oscillations are limited to the neighborhood of x_3^e and the other in which the oscillations are over the entire interval $[0, 6]$. Concerning the red diagram for the k -monopolist, the optimal output proceeds to chaotic oscillation through a typical period-doubling bifurcation cascade for $\tau \leq \tau_1^K \simeq 1.07$. The periodic cycles appear again for $\tau > \tau_1^K$, and their domains are extended. For the blue diagram for the ℓ -monopolist, differ-

¹³It is to be noticed that the two-delay equation (17) is defined for $\tau_1 \leq \tau_2 = 3$ whereas the one-delay equation (18) does not have such a restriction and can be defined for $\tau > 3$ as well.

ent dynamic transition is observed with respect to τ_1 . In the first phase for $\tau_1 < \tau_a^L \simeq 1.43$, a period-2 cycle is basic and its variants emerge. At the near-end of the first phase, chaotic oscillations suddenly arise. In the second phase for $\tau_1 > \tau_a^L$, chaotic oscillation expands its domain including x_1^e . The blue diagram has a window in which periodic oscillations arise for $\tau_1 > \tau_b^L \simeq 2.11$. Chaotic oscillations appear again for τ_1 getting closer to 3. Returning to the definitions of $g(x_1(t - \tau_1), x_2(t - \tau_2))$ and $f(x(t - \tau))$, we see that

$$\lim_{\tau_i \rightarrow \tau_j} g(x_1(t - \tau_1), x_2(t - \tau_2)) = f(x_j(t - \tau_j)) \text{ for } i, j = 1, 2 \text{ and } i \neq j.$$

This equality implies that the two-delay model (17) converges to the one-delay model (18) when one delay τ_j of (17) is fixed and the other delay τ_i gets closer to τ_j . Hence in the neighborhood of $\tau_1 = 3$, both delay equations (17) and (18) generate similar dynamics, very complicated dynamics in our example.

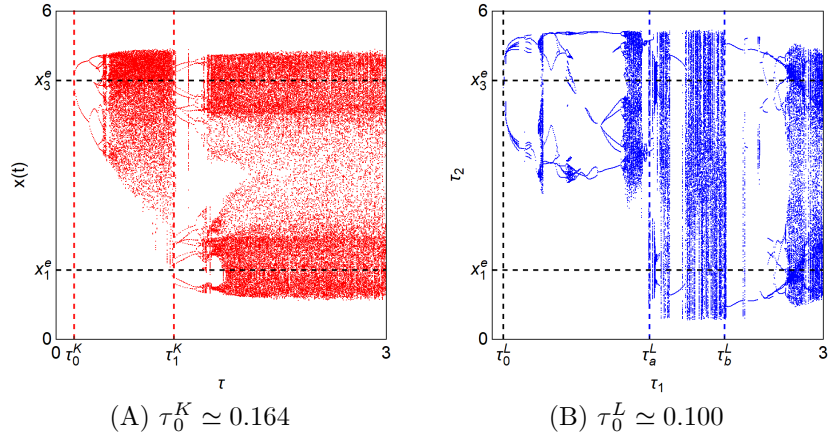


Figure 12. Bifurcation diagrams with respect to τ and τ_1

Figure 13 depicts phase diagrams for three different values of bifurcation parameters τ and τ_1 in which the blue and red trajectories are represented, respectively, by (17) and (18). For $\tau = \tau_1 = 0.4$, both equations generate periodic solutions as shown in Figure 13(A) in which equation (17) produces a blue limit cycle and equation (18) a red multiperiodic cycle. The phase trajectories starting for $\varphi(t) = x_3^e + 0.1$ are illustrated in the upper-right corner. Figure 13(A) also displays symmetric diagrams with respect to $x = x_2^e$ in the lower-left corner. These cycles are obtained under the different initial function, $\varphi(t) = x_1^e + 0.1$. For the smaller bifurcation values, the delay equations have initial point dependency. In Figure 13(B) the values of the bifurcation parameters are increased to $\tau = \tau_1 = 1.2$. It is seen that the k -monopolist's dynamics exhibits global oscillations, that is, the trajectory oscillates around x_3^e for a while, then moves to the neighborhood of x_1^e oscillating there. Soon later, it is

back to the x_3^e -neighborhood again. These ups and downs are repeated. On the other hand, the ℓ -monopolist's dynamics is confined to the neighborhood of the equilibrium output. The neighborhood where it stays depends on which initial function the dynamic equation adopts. The dynamics with a larger τ_1 -value is more complicated than the one with a lower τ_1 -value. For $\tau = 1.8$, the lower oscillation and the upper oscillation are merged to make chaotic global oscillation including two stationary outputs, x_1^e and x_3^e as shown in Figure 13(C).

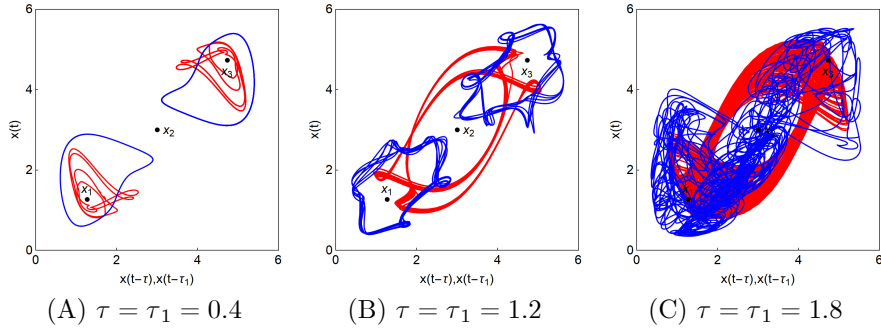


Figure 13. Comparison between phase diagrams of two monopolists

5 Concluding Remarks

Rational monopolies have exact knowledge on the price function and have enough computability to find the profit maximizing output level, which is then known instantaneously giving no need for dynamic adjustments. Boundedly rational monopolies either know the price function but do not have the sufficient computability to find the profit maximizing output level or they can observe only output and price data from previous time periods. In the first case the usual gradient adjustment process is applied and its delay version gives a one-delay model. In the second case the marginal profit is approximated with a two-point finite difference formula leading to a two-delay model. Assuming discrete time scales, the stability conditions are identical requiring sufficiently small speed of adjustments, however, the dynamics of the two models show some differences. The case of continuous dynamics is different. In the one delay case the critical values of the delay are computed and the directions of stability switches are determined via Hopf bifurcation. In the two delay case the discrete model is transformed into a continuous model based on the Berezowski transformation. The stability switching curves are analytically determined and the directions of stability switches are characterized based on the value of the stability index at each point of the curves. The theoretical results are verified and illustrated by numerical studies, In cases of stable and unstable steady states the dynamics is illustrated and sensitivity analysis is performed. It is shown that the speed of

adjustments has a destabilizing effect while the inertia coefficient has a stabilizing effect.

The study reported in this paper can be extended in several directions. First, more complex forms of the price function can be included in the model and to show how the dynamics depends on function forms and parameters. Second, to avoid sudden market fluctuations, a linear combination of previous output values can replace the most current output level leading to multiple delay systems. Third, the gradient adjustment process can be changed to other dynamic schemes. In the gradient process the profit maximizing output is approximated with a first-order formula, however, higher-order formulas are also known from the literature, which can be included in the dynamic equations.

References

- [1] Askar, S., On complex dynamics of monopoly market, *Economic Modelling*, 31, 586-589, 2013.
- [2] Berezowski, M, Effect of delay time on the generation of chaos in continuous systems: One-dimensional model, two-dimensional model-tubular chemical reactor with recycle, *Chaos, Solitons and Fractals*, 12, 83-89, 2001.
- [3] Elsadany, A., and Awad, A., Dynamical analysis of a delay monopoly game with a log-concave demand function, *Operations Research Letters*, 44, 33-38, 2016.
- [4] Gu, K., Niculescu, S-I., Chen, J., On stability crossing curve for general systems with two delays, *Mathematical Analysis and Applications*, 311, 231-253, 2005.
- [5] Hicks, J. R., Annual survey of economic theory, *Econometrica*, 3, 1-20, 1935.
- [6] Matsumoto, A. and Szidarovszky, F., Delay Cournot duopoly game with gradient adjustment: Berezowski transition from a discrete method to a continuous method, *Mathematics*, 9, 32, <https://doi.org/10.3390/math9010032>, 2021.
- [7] Matsumoto, A. and Szidarovszky, F., Delay dynamics in nonlinear monopoly with gradient adjustment, *IERC DP 341*, Institute of Economic Research, Chuo University, 2021.
- [8] Matsumoto, A. and Szidarovszky, F., *Dynamic Oligopolies with Time Delays*, Springer-Verlag, Singapore/Tokyo, 2018.
- [9] Matsumoto, A., and Szidarovszky, F., Discrete and continuous dynamics in nonlinear monopolies, *Applied Mathematics and Computation*, 232, 632-642, 2014.
- [10] Naimuzada, A., and Ricchiuti, G., Complex dynamics in a monopoly with a rule of thumb, *Applied Mathematics and Computation*, 203, 921-925, 2008.
- [11] Puu, T., The Chaotic Monopolist, *Chaos, Solitons and Fractals*, 5, 35-44, 1995.
- [12] Robinson, J., *Economics of Imperfect Competition*, Macmillan, London, 1933.
- [13] Rustichini, A., Hopf bifurcation for functional differential equation of mixed type, *Journal of Dynamics and Differential Equations*, 1, 145-177, 1989.